Atmos. Meas. Tech., 5, 2969–2980, 2012
www.atmos-meas-tech.net/5/2969/2012/
doi:10.5194/amt-5-2969-2012

Atmospheric Measurement Techniques

XCO_2-measurements with a tabletop FTS using solar absorption spectroscopy

M. Gisi[1], F. Hase[1], S. Dohe[1], T. Blumenstock[1], A. Simon[2], and A. Keens[2]

[1]Karlsruhe Institute of Technology (KIT), Institute for Meteorology and Climate Research (IMK-ASF), Karlsruhe, Germany
[2]Bruker Optics GmbH, Ettlingen, Germany

Correspondence to: M. Gisi (michael.gisi@kit.edu)

Received: 24 July 2012 – Published in Atmos. Meas. Tech. Discuss.: 17 August 2012
Revised: 24 October 2012 – Accepted: 3 November 2012 – Published: 29 November 2012

Abstract. A commercial low-resolution ($0.5\,cm^{-1}$) Fourier Transform Spectrometer (FTS) has been modified and is used for determining the total column XCO_2 of the atmosphere by analysing direct solar radiation. The spectrometer has a small home-built solar tracker attached, so that it is a ready-to-use instrument. The results are validated with temporally coinciding on-site measurements taken with a high-resolution Total Carbon Column Observing Network (TCCON) FTIR spectrometer. For the whole comparison period of 5 months (26 measurement days) an agreement with TCCON results of $(0.12 \pm 0.08)\,\%$ is achieved. This makes the spectrometer a promising candidate for a low-cost addition to the TCCON core FTIR sites, especially suitable for locations with limited infrastructure. An impressive mechanical and thermal stability is proved, enabling the spectrometer for use in field campaigns and for the monitoring of local sources.

1 Introduction

Within the last several years, it has been recognised that a precise knowledge of the global abundances of greenhouse gases such as CO_2, N_2O and CH_4 is required for understanding the mechanisms of the global carbon cycle and to determine it's sources and sinks (Olsen and Randerson, 2004). To measure column-averaged mole fractions of these gases, several satellite-borne instruments were developed such as SCIAMACHY (http://www.sciamachy.de/), GOSAT (http://www.gosat.nies.go.jp/index_e.html) and OCO/OCO-2 (http://oco.jpl.nasa.gov/news/). The latter two missions are exclusively dedicated on measuring greenhouse gases and OCO-2 is scheduled for launch in 2014. To support and validate these measurements great efforts have been undertaken to set up the Total Carbon Column Observation Network (TCCON). It consists of 23 globally distributed, ground-based solar absorption Fourier transform spectrometers operating in the Near Infrared (NIR) spectral region to measure the CO_2 total column in the atmosphere. These high-resolution TCCON spectrometers achieve an unprecedented accuracy of 0.25 % for the atmospheric XCO_2 content (Wunch et al., 2011). The XCO_2, which is the column-averaged dry-air mole fraction, is derived by the ratio of the measured CO_2 and O_2 total columns by

$$XCO_2 = \frac{CO_{2,\mathrm{column}}}{O_{2,\mathrm{column}}} \cdot 0.2095 \quad (1)$$

where 0.2095 is the dry air O_2 mole fraction. This approach compensates for numerous systematic errors, such as a pointing offset or an erroneous surface pressure. To make the network results comparable to WMO (World Meteorological Organisation) standards, the retrieved XCO_2 value is divided by a calibration factor of 0.989. This value was determined by comparisons with in situ profiles measured in the framework of aircraft campaigns (Wunch et al., 2010; Messerschmidt et al., 2011).

Despite its outstanding capabilities such as the precision and stability during normal operations, the IFS125HR spectrometers from Bruker™ used by the TCCON also have their limitations. The IFS125HR is an expensive high-precision instrument, its large dimensions on the order of $1 \times 1 \times 3\,m$ and the mass well beyond 100 kg makes it difficult to transport, and its operation requires a significant amount of infrastructure, such as a stable support platform, air conditioning and sufficiently large lab space. For regular maintenance

such as realignment and for repairs, an experienced person has to access the instrument, which can be difficult and time-consuming. The IFS125HR is not a portable spectrometer, moving it to a new site requires time-consuming start-up procedures. These obstacles impede the scientifically important ground-based extension of atmospheric carbon column measurement on a global scale, e.g., in Africa and South America.

Some flexibility is gained by integrating the spectrometer into an overseas container including air conditioners and solar trackers (Geibel et al., 2010). But still, a truck and a forklift have to be available as the containers measure about 15 ft (4.57 m) and weigh several tons. For field campaigns and for operation in remote areas with low infrastructure (the power consumption of such a container is on the order of 5 kW), this approach is hardly manageable.

To overcome these problems, the usage of smaller, cheaper and more easily transportable spectrometers was recently investigated to asses the ability to measure XCO_2. Besides the ability to be used easily in field campaigns, assuming a sufficient compactness and mechanical stability, the spectrometers could even be sent back and serviced by the manufacturer or the staff of the home institution for repairs or realignments, reducing the costs and effort significantly. A robust instrumentation which can be operated in a wide range of ambient temperatures would promote global deployment.

One alternative is the IFS125M instrument, which is smaller and less sturdy than the IFS125HR, while offering comparable resolution. Due to its lightweight design, the stability of the instrumental line shape (ILS) is not at the level of the IFS125HR spectrometer, so that it is difficult to achieve the long-term stability required by TCCON (V. Sherlock, NIWA, personal communication, 2012). In addition, it still has a length of about 2 m and requires on-site realignment by qualified personnel. The IFS125M spectrometer has been successfully operated on ships (Notholt et al., 2000).

In addition, several compact and medium-to-low-resolution instruments currently are under investigation, such as a grating spectrometer (about 0.16 cm^{-1} resolution), a fiber Fabry-Perot interferometer (both setups presented in Kobayashi et al., 2010), the IFS66 from Bruker (0.11 cm^{-1}) (Petri et al., 2012), a Nicolet Spectrometer from Thermo-Scientific (0.125 cm^{-1}) (Chen et al., 2012) and the IR-Cube from Bruker (0.5 cm^{-1}) (Jones et al., 2012).

In this work, we demonstrate for the first time the suitability of a very compact setup, consisting of a modified commercial FTS with a resolution of 0.5 cm^{-1} and a miniature solar tracker attached to it. We verify the long-term stability, present the tracker setup and the modifications applied to the commercial spectrometer to achieve XCO_2 measurements with a precision of 0.08 % over several months, validated with respect to a co-located TCCON spectrometer.

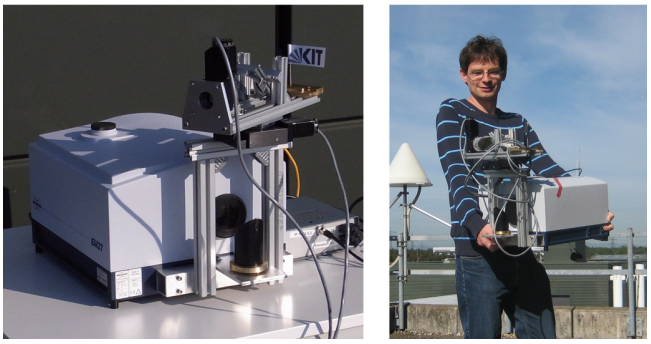

Fig. 1. The EM27 Spectrometer with the attached tracker. Right panel: transportation to the roof of the building where the measurements were made.

2 Instrumentation

Our aim was to investigate the capabilities of a compact and robust spectrometer, which is sufficiently small and light to be carried by one person, without compromising the ability to align, modify and check internal optical components due to the compactness. In addition, we developed a small and transportable solar tracker which is directly attached to the spectrometer. This merged setup, which is displayed in Fig. 1, is ready to use for various kinds of environmental research measurements.

2.1 Home-built tracker

The target requirements for the tracker were to reach a high tracking precision with a compact and lightweight setup. We decided to realise an alt-azimuthal tracker, with 2 stepper motor driven rotation stages. The complete tracker weighs about 2 kg and has the dimensions $30 \times 20 \times 10$ cm. It supports a beam diameter of 50 mm, which actually is much wider than required for the purpose described in this paper, as only a beam diameter of 3 mm is used for the solar absorption measurements (see Sect. 2.2). However, this fact allows application of the tracker kinds of observations (e.g., lunar, open path, emission measurements). We used 2 rotation stages with hollow axes from Standa (http://www.standa.lt).

They are driven by stepper motors controlled by the "SMCI12" motor drivers from Nanotec (http://www.nanotec.com), allowing a microstep size of 1/64th of a full step, which results in a theoretical 0.56 arc seconds resolution along both axes. The mirrors are elliptic glass plates with SiO_2 protected aluminum coating.

The tracker is controlled by our CamTracker approach, so the optical tracking feedback is derived from a camera recording the field stop of the spectrometer, leading to very consistent control of the spectrometer's line of sight. Technical details are given in Gisi et al. (2011). A camera image of the illuminated aperture is shown in Fig. 2.

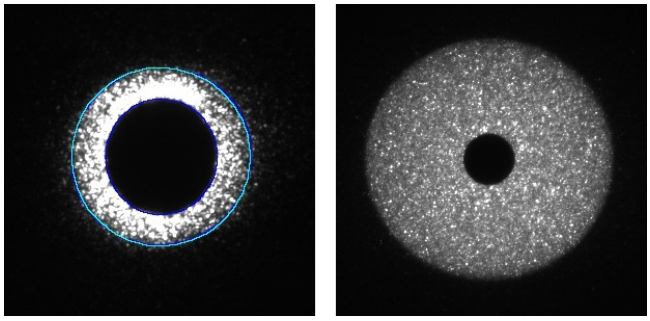

Fig. 2. Images of the solar disk on the field stop of the EM27 spectrometer (left panel) and the IFS125HR in Karlsruhe (right panel) as recorded by CamTracker. The blue circles in the left image are the outlines, as they are detected and used by the CamTracker program for maintaining and correcting the precision of the tracking. The field-of-view differs between the EM27 and the IFS125HR.

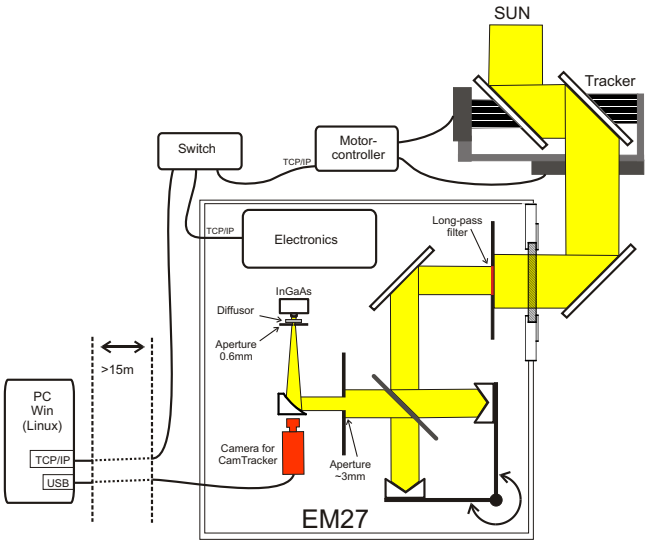

Fig. 3. Schematic drawing of our measurement setup and the EM27 spectrometer. The camera is not in the same plane as the mirror, instead it observes the field stop by a small angle from above.

2.2 The NIR-modified EM27 spectrometer

We decided to use the EM27™ spectrometer from Bruker. This spectrometer uses the RockSolid™ pendulum interferometer with 2 cube corner mirrors and a CaF_2 beamsplitter, which offers very high stability with respect to thermal and mechanical disturbances. The interferometer supports a beam diameter of 40 mm. The pendulum is attached by springs, resulting in frictionless and wear-free movements. This principle results in even higher reliability of the interferometer in comparison to the 125HR setup. The latter suffers from wear due to use of friction bearings on the linearly moving retroreflector. This wear introduces a shear misalignment and requires regular realignment (Hase, 2012).

The EM27 achieves 1.8 cm optical path difference equivalent to 0.5 cm^{-1} resolution. To realise this, the retroreflectors of the pendulum structure move a geometric distance of 0.45 cm. The sampling of the interferogram is controlled by a standard, not frequency-stabilised HeNe laser. The sealed spectrometer compartment contains a desiccant cartridge; the radiation enters through a wedged fused silica window. So the spectrometer withstands and can be operated in adverse environmental conditions, e.g., high relative humidity. It measures approximately $35 \times 40 \times 27$ cm and weighs 25 kg including our home-built tracker. Due to the current electronics, with a resolution of 0.5 cm^{-1}, the spectrometer is capable of recording single-sided interferograms only, however, an electronics update will overcome this limitation in the future. It is compact enough to be carried by one person, but still offers sufficient space inside for modifications and alignments of the light path, allowing us to test various setups.

A schematic drawing of the EM27 with modifications is presented in Fig. 3. The tracker, which was described in Sect. 2.1, leads the solar radiation into the EM27 spectrometer. We limit the beam to 25 mm free diameter by using a 750 nm long-pass-filter a few centimetres behind the entrance window in order to block unwanted radiation which would disturb the laser detectors of the interferometer.

After the radiation has passed the interferometer, it is blocked by an aperture (which forms the aperture stop of the optical system) with a diameter of 3 mm. We inserted this aperture for controlling optical aberrations (to achieve a near-theoretical instrumental line shape, see Sect. 3.1) and for avoiding nonlinear detector response. The remaining part of the radiation is appropriate for recording solar absorption spectra. Finally the beam is focused on a field stop with 0.6 mm diameter by a 90 ° off-axis paraboloid with an effective focal length of 101.6 mm. In combination, this results in a semi Field-of-View (FOV) of 2.96 mrad. This is half of the angle subtended by the FOV. The field stop is inclined versus the optical axis by a few degrees to avoid channelling. As partially illuminated detectors show unwanted nonlinear and ILS effects, a diffuser was placed between the field stop and the InGaAs detector (size $1 \times 1\,mm^2$, spectral sensitivity 6000–9000 cm^{-1}). The detector signal is DC coupled, allowing corrections for solar intensity variations due to thin clouds (Keppel-Aleks et al., 2007).

The image of the sun on the field stop is recorded by the camera which then is used as the optical feedback for the tracker (CamTracker), as described in Gisi et al. (2011). This is a very precise method for controlling the actual line of sight of the spectrometer. Changes of the alignment of any mirror, e.g., during transportation, have no effect on the accuracy of the tracking and the resulting line of sight. An image of the sun on the aperture as it is recorded by the camera is shown in Fig. 2.

The tracker and the EM27 interferometer are connected to a controlling computer via a standard network cable. The

USB cable of the camera uses a separate outlet of the housing of the spectrometer and is connected with a 15 m active USB extension cable to the computer.

The controlling computer is equipped with an Intel 3.2 Ghz processor, runs Windows 7, the operating software for the spectrometer (Opus 7) and the CamTracker program. It was located one floor below the terrace on which we placed the EM27 spectrometer.

3 Characteristics

3.1 Instrumental line shape

Any quantitative trace gas retrieval depends on a proper knowledge of the spectral degradation characteristics. For FTIR spectrometers this instrumental line shape (ILS) is advantageously separated into one part which refers to the inherent self-apodization of an FTS with circular field stop and, therefore, also exists for an ideally aligned spectrometer. This contribution can be calculated easily using the spectrometer's field-of-view and the optical path difference of the interferometer. The second component of the ILS can be described by a complex modulation efficiency (represented by a modulation amplitude and a phase error, both functions of optical path difference) which result from misalignments and optical aberrations. These parameters have to be derived by experiment, e.g., by evaluating gas cell measurements (Hase et al., 1999).

A standard approach for the high-resolution FTIR instruments is to use low-pressure gas cells. We checked the ILS of the EM27 by measuring the water vapour lines of about 2 m in ambient air using a collimated standard halogen bulb as light source. This minimalistic approach makes a gas cell obsolete and can easily be performed, e.g., during measurement campaigns. To analyse these results and to obtain the modulation efficiency and the phase error, we used the version 12 of the LINEFIT program (Hase et al., 1999). The required parameters for the correct interpretation of the spectrum are the ambient temperature, the total pressure and the partial water pressure (the latter is a by-product of the LINEFIT analysis).

We performed these measurements twice within the time series presented in this paper. On 8 February 2012 and 22 May 2012 the derived modulation efficiencies at maximum optical path difference were 0.9954 and 0.9910, respectively. However, as the water vapour lines in HITRAN which we used contain inaccuracies, the absolute value for the derived modulation efficiency and the phase error depend on the selected spectral range. Therefore, we can only conclude that the ILS of the EM27 is impressively stable, but the absolute calibration of the modulation efficiency requires further study of the H_2O line parameters in the 7000 cm^{-1} spectral region.

For our system with a spectral resolution of 0.5 cm^{-1} an increase of 1 % of the modulation efficiency results in an XCO_2 increase of 0.15 %. As in our time series the assumed modulation efficiency changed by less than 0.5 %, we used a constant ideal ILS in our retrievals. Note that no realignment of the spectrometer was performed over the whole period, although the spectrometer was transported frequently and was exposed to temperatures between −10 and +40 °C. We estimate that our knowledge of the absolute modulation efficiency is within 2 %, which implies that the systematic offset between the EM27 and 125HR XCO_2 timeseries should be below 0.3 %.

3.2 Ghost to parent ratio

For the recording of NIR spectra in the 6000 to 9000 cm^{-1} range, the interferogram (IFG) sampling has to be performed at each rising and falling zero crossing of the laser AC signal. This makes the IFG recording prone to alternating sampling errors, which generates artifacts (ghosts) in the spectral domain, as described in detail by Messerschmidt et al. (2010). As this problem affected several TCCON measurement sites in the past, we decided to check the GPR (ghost-to-parent ratio) for our setup.

In contrast to the IFS125HR spectrometers, it is not possible to readjust the GPR with the currently available EM27 electronics. The laser-detecting photo diodes, however, are the same as used in the latest 125HR version.

With our EM27 spectrometer we measured a GPR of 2×10^{-4} which is of the order of the current TCCON recommendations (1×10^{-4}). F. Hase recently suggested an IFG resampling scheme which has been successfully applied for correcting interferograms collected by different TCCON spectrometers (S. Dohe, KIT, personal communication, 2012; V. Sherlock, NIWA, personal communication, 2012). For the EM27, we refrained from performing any correction because the GPR is rather small.

4 Measurements and analysis

4.1 Setup and operation of the spectrometers: EM27 and reference TCCON spectrometer

We operated the EM27 spectrometer on the roof terrace of our office building at 133 m a.s.l. with the coordinates 49.094° N and 8.4336° E. The testing period covered 26 measurement days from 3 February 2012 to 22 June 2012. For each day of operation, the spectrometer was moved from its storage place in the fourth floor to the terrace on floor 7, see Fig. 1. As we used a simple unsprung trolley for transportation, the spectrometer was subject to significant mechanical vibrations. When placing the spectrometer outside, we did not put much effort into a precise leveling or orientation. A coarse orientation relative to the wall of the building was sufficient to enable the CamTracker programme to detect the sun on the field plane and to centre it to the field stop (see Fig. 2). During operation, the spectrometer experienced

outside ambient conditions. Temperatures in February were as low as −10 °C, in May the spectrometer was heated to temperatures above 40 °C due to exposure to direct sunlight. We alternately recorded single-sided interferograms with 0.5 cm^{-1} and double-sided interferograms with 1 cm^{-1} resolution, with 10 averages each. The recording time for each of these measurements (being an average of 10 IFGs) was about 34 s. The applied scanner speed was 10 kHz. For the further analysis in this work we only evaluated the 0.5 cm^{-1} resolution measurements, because a significant loss in contrast between the CO_2 lines and the adjacent continuum is observed when the resolution is reduced to 1.0 cm^{-1}, as can be seen in Fig. 4. We chose the alternately 0.5 cm^{-1} and 1 cm^{-1} recording scheme, to maintain the option for evaluating the spectrometer's capabilities with 1 cm^{-1} resolution, and to check for differences in the single-sided and double-sided recording scheme. However, as we only evaluated the 0.5 cm^{-1} resolution spectra, the effective duty-cycle of the EM27 is only 50 %.

The TCCON instrument in Karlsruhe located about 700 m north of our office building at 110 m a.s.l. at the coordinates 49.100° N and 8.4385° E provided the reference XCO_2 dataset. During each of the 26 EM27 measurement days, 125HR spectra were recorded in parallel.

In addition, various meteorological observations are available at the site. In our context, the records of ground pressure and tall tower temperatures at 100 and 200 m altitude are of relevance. These auxiliary data have been used for the analysis of the spectra (see Sect. 4.2). The ground pressure sensor is a BM35-barometer from meteolabor™ with a stated accuracy of ±0.05 hPa. The temperature is acquired from a PT100 sensor (Type 2015) from the company "Theodor Friedrichs & Co". It's accuracy is stated as $0.1\,°C + 0.005 \cdot T$, with T in degrees Celsius.

4.2 Data processing and evaluation

The official analysis code for the TCCON network is GFIT. GFIT is maintained by G. Toon at the California Institute of Technology and used by the TCCON as a part of the software package GGG, which also includes preprocessing of the interferograms and post-processing of the resulting XCO_2. More details can be found in Wunch et al. (2011). However, we preferred to use our own calibration tools and retrieval code PROFFIT Version 9.6 for the EM27 study. Our setup is well established for work within the NDACC FTIR network and has been validated in various studies (Schneider et al., 2008, 2010; Sepúlveda et al., 2012). Therefore, we will first show that our setup well reproduces the official TCCON 125HR XCO_2 results for the high-resolution 125HR spectra, where the 2012 software release including the April update was used. Next, we analyse the EM27 spectra and resolution-reduced 125HR spectra with our retrieval setup. The resolution-reduced 125HR spectra have been included

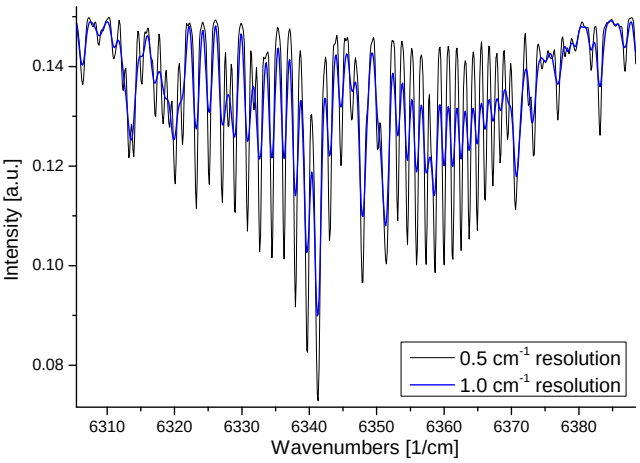

Fig. 4. A section of the CO_2 retrieval window with 0.5 and 1 cm^{-1} resolution. A Norton-Beer apodization function was applied to the interferogram to suppress sidelobes next to each spectral line, which is an artifact in low-resolution FTIR spectra.

to discern instrumental effects from apparent XCO_2 changes when analysing low-resolution spectra.

We used the same O_2 line list and the same CO_2 and H_2O a priori mixing ratio profiles as used by the official TCCON analysis. For CO_2 we used the HITRAN08 lines and an own line-mixing parameterisation scheme. The required line-mixing parameters were derived from a code provided by J.-M. Hartmann (Lamouroux et al., 2010).

The pressure and temperature profiles for all PROFFIT evaluations were taken from local meteorological measurements (ground pressure and tall tower temperatures at 100 and 200 m altitudes) and the MERRA (Modern-era retrospective analysis for research and applications) model data "IAU3D assimilated state on pressure(inst3_3d_asm_CP)" (http://disc.sci.gsfc.nasa.gov/daac-bin/DataHoldings.pl). Besides other parameters, this provides the temperature and pressure on a 1.25×1.25 ° grid, from 1000 to 0.1 hPa for 8 times per day.

For each of these times, the solar position is calculated and the pressure and temperature values along the unrefracted path of the solar radiation are retrieved from the model data. These profiles are then used as an input for the PROFFIT retrieval. The profile which is used for the evaluation of a spectrum recorded at a specific time is calculated by PROFFIT by applying a linear interpolation between two temporally adjacent profiles.

No post-processing of the XCO_2 results has been performed within our analysis sequence apart from applying the TCCON calibration factor of 0.989 (Wunch et al., 2010) to all XCO_2 results. In accordance with previous studies (Petri et al., 2012), we find that reducing the spectral resolution significantly below the resolution applied by the TCCON network leads to a systematic increase of the retrieved O_2 and CO_2 columns. The study by Petri et al. (2012) was performed

using GFIT, we observe similar – but not identical – changes with our independent analysis setup. Therefore, we assume that this effect is partly introduced by deficiencies of the far-wing line shape model and partly stems from approximations of the line-by-line calculation of absorption cross-sections. Anyway, such a systematic offset can be removed by adjusting the XCO_2 calibration factor for a hypothetical EM27 network.

We processed and evaluated the data in 4 different ways which will later be denoted as "EM27", "HR_High", "HR_Reduced" and "GFIT":

- "*EM27*": PROFFIT-evaluated averages 10 IFG of EM27 with 0.5 cm^{-1} resolution. The IFGs were apodized by a Norton-Beer-Medium function.
- "*HR_High*": PROFFIT-evaluated averages of 4 IFGs (2 forward, 2 backward) from TCCON instrument with 0.014 cm^{-1} resolution.
- "*HR_Reduced*": The initial measurements are the same as in "HR_High", but the interferograms were truncated to 0.5 cm^{-1} resolution and apodized by a Norton-Beer-Medium function. The retrieval scheme then was the same as described in "EM27".
- "*GFIT*": GFIT-evaluated averages of 2 forward or 2 backward interferograms of the TCCON instrument with 0.014 cm^{-1} resolution (forward and backward interferograms are analysed separately). For the time-series intercomparison in Sect. 5.3, these separate forward- and backward results are averaged, in contrast to the figures containing the gas columns and the XCO_2-values in the course of measurement days. In any presented data, we applied the IFG preprocessing routines from GGG (correction of solar intensity variations and determination of the phase spectrum used for the FFT), as described in Wunch et al. (2011). For the calculation of XCO_2 values we applied the standard GFIT post-processing routines. These include an averaging of the 2 CO_2 column values as two separate spectral windows are evaluated (see Sect. 4.3). In this averaging, a multiplicative bias between the 2 spectral windows is corrected for, which is determined from the whole available dataset. In the next step, the XCO_2 values are calculated according to Eq. (1) and an empirical airmass-dependent correction factor is applied. Further details can be found in (Wunch et al., 2011) and on the TCCON wiki webpage https://tccon-wiki.caltech.edu.

The "*EM27*" and "*HR_Reduced*" low resolution spectra were generated from the interferograms after applying the Norton-Beer-Medium function. In low-resolution spectra, omitting the numerical apodization would introduce significant sidelobes around all spectral lines. As these fade away slowly, modelling of these artifacts would complicate the calculation of the model spectra considerably. The Norton-Beer-Medium apodization is a good compromise between sufficiently effective suppression of sidelobes and degradation of spectral resolution.

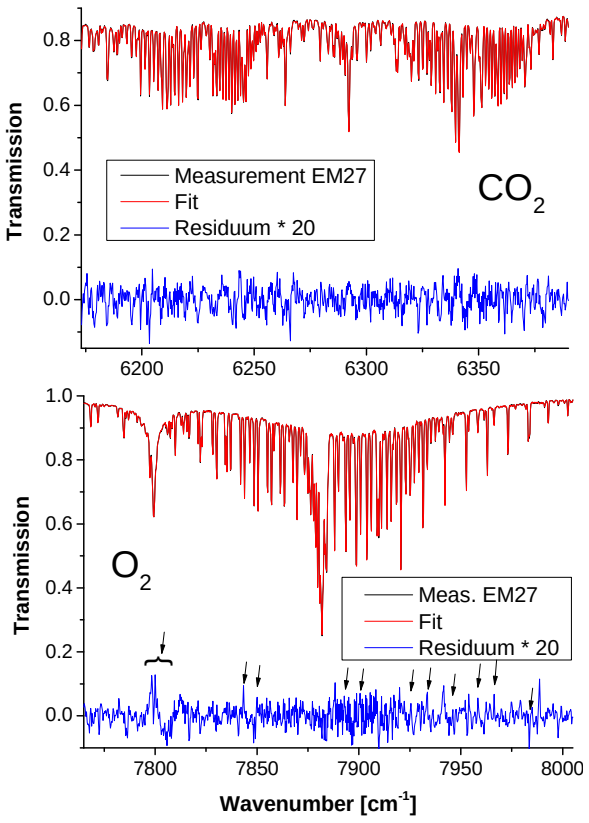

Fig. 5. Spectral windows used by PROFFIT to derive the CO_2 and O_2 columns. In the lower figure the systematically occurring residuals due to deficiencies of the solar line modelling are marked in the residual.

4.3 Spectral windows

In the official TCCON analysis, the CO_2 column is evaluated in the spectral ranges 6180–6260 and 6297–6382 cm^{-1}, for the O_2 analysis the range 7765–8005 cm^{-1} is applied. For the PROFFIT analysis of the 125HR and EM27 spectra, we adopted the same O_2 window, but we merged the CO_2 windows into one broader region extending from 6173 to 6390 cm^{-1}.

An example of the spectral windows including the measurement, the fit and the residual is presented in Fig. 5. For both windows, the quality is very good and the standard deviation of the residual is $1\sigma = 0.2\,\%$ for CO_2 and 0.17 % for O_2. However, several peaks appear in the EM27 residuals (in the graph of the O_2 marked with arrows) which do not appear in the resolution-reduced 125HR spectra.

These residuals originate from the fact that the intensity and shape of the solar lines vary as function of the projected solar disc radius (Hase et al., 2006). Because the FOV of

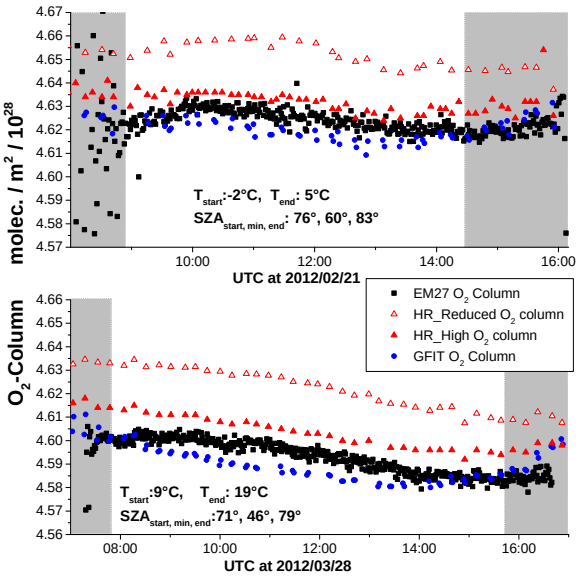

Fig. 6. O_2 columns for the four datasets for two sample days. The observed intraday variability is very low. The number of interferograms and respective recording interval contained in a single datapoint of each type are the following: EM27: 10 IFGs, 34 s; HR_Reduced: 4 IFGs, 34 s; HR_High: 4 IFGs, 212 s; GFIT: 2 IFGs, 106 s.

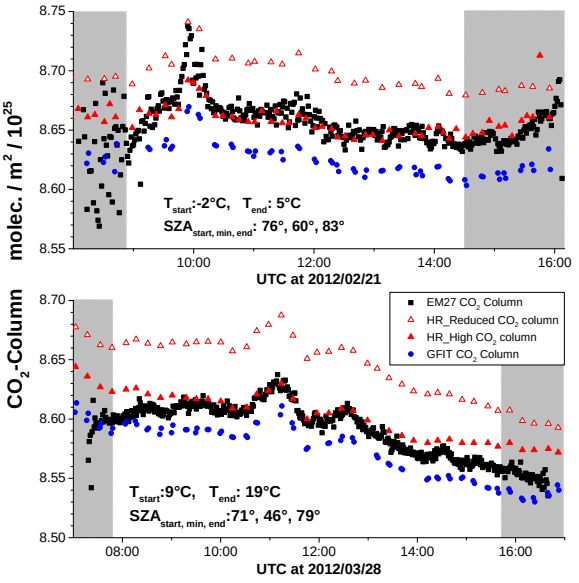

Fig. 7. CO_2 columns for 2 days. The systematic offsets of the 4 datasets is very similar to those in the O_2-columns. The number of interferograms and respective recording interval contained in a single datapoint of each type are the same than in Fig. 6

the EM27 instrument of 2.95 mrad (semi-FOV) is a factor of about 3 greater compared to the one of the IFS125HR, which has a semi-FOV of 0.957 mrad, the EM27 observes a significantly larger fraction of the solar disc. An image of the solar disc superimposed on the field stop as recorded by the Camtracker is displayed in Fig. 2. The current NIR line list used by PROFFIT does not include parameters to describe the centre-to-limb variability of the solar lines.

5 Results

In this section, we evaluate the results for the EM27 in comparison to the 125HR reference. In Sects. 5.1 and 5.2 we provide an overview of the CO_2 and O_2 columns and the resulting intraday variability of XCO_2 during several sample days. In Sect. 5.3, a statistical analysis for the whole set of measurements is provided.

5.1 CO_2 and O_2-columns

Figures 6 and 7 show the O_2 and CO_2 columns for the measurement days 21 February 2012 and 28 March 2012. In each graph, the ambient air temperature on the terrace is given for the beginning and the end of the EM27 measurements. In addition, the starting, the minimal and the last value for the solar zenith angle (SZA) of the measurements are displayed. The values in the areas with a gray background are not taken into account in the statistical analysis of Sect. 5.3. The shaded areas filter out SZAs beyond 70 ° and measurements taken within the first 30 min after the start of measurements. We added the latter restriction as the EM27 requires some startup time before it operates in a stable manner. After moving it from the 20 °C lab environment to the outside temperature on the terrace, which was sometimes as low as −12 °C, the HeNe reference laser tube temporarily undergoes fast temperature changes, thereby shifting the reference wavelength during a few scans.

Columns for O_2 recorded on 2 days are presented in Fig. 6. The data processing procedure for the 4 types of datapoints were described in Sect. 4. One observes a difference between the "HR_High" and the "HR_Reduced" columns, resulting from the reduction of the resolution. The "HR_Reduced" columns of O_2 are 0.4 % higher than the reference values. This systematic resolution-depending difference was also observed before by Petri et al. (2012). Possible reasons for this discrepancy are discussed in Sect. 4.2. A closer inspection reveals that this is not a constant correction factor in case of the CO_2 column, but also a weaker airmass-dependent contribution can be observed. The "HR_Reduced" CO_2 columns are 0.4 to 0.6 % higher than the reference values. This finding is not surprising for an effect probably induced by line-shape issues. Nevertheless, this is not an obstacle for a hypothetical EM27 network, but a matter of adjusting the analysis procedures, as the TCCON network also performs some air mass dependent tuning in the course of the analysis of the 125HR spectra.

One would expect the EM27 O_2 and CO_2 columns to reproduce the "HR_Reduced" values. However, despite using

the same retrieval parameters, we observe values approximately 0.6 % lower. We are not sure about the origin of this offset, as the retrieval scheme (a prioris, pressure and temperature profiles, used resolution,...) is exactly the same. As outlined in Sect. 3.1 the absolute ILS calibration of the EM27 might be slightly off, and the observed discrepancies are within the resulting error bar (moreover, the offset is nearly the same for CO_2 and O_2 columns as one would expect in this scenario). Therefore, we assume that the uncertainty of the ILS calibration is the leading effect. In addition, the deficiencies of the solar line model could trigger parts of the systematic offsets. The variation in the EM27 O_2 columns during the evaluated days is very low which proves the high stability of the EM27 spectrometer as well as the high performance of the CamTracker system. When comparing the "GFIT" and "HR_High" results generated with PROFFIT, one observes an air mass dependent increase of the GFIT values. For this reason, the TCCON applies a posteriori airmass correction to the XCO_2 values. For the PROFFIT evaluated O_2 columns this effect is not evident, although the same line lists are used.

When compared to the intraday variability of the O_2 columns, the higher variability of the CO_2 columns is obvious. These enhancements are indicated by both the EM27 and the 125HR and are discussed in Sect. 5.3.

5.2 XCO_2

The XCO_2 values for 5 sample days are presented in Fig. 8. As described in Sect. 4.2, all datasets are calculated by Eq. (1) and include the WMO calibration factor of 0.989. In addition, the GFIT(TCCON) dataset contains a GFIT-specific post-correction, especially an air mass dependent correction.

Obviously the systematic differences between the 4 datasets cancel out very well so that they agree within about 1 ppm. The intraday variability differs strongly between the measurement days. During some days the values vary very smoothly (e.g., 22 March 2012), others, such as the 28 March 2012, show several short-term increases. As these are observed both by the EM27 and the 125HR and the simultaneously recorded CamTracker images look unsuspicious, we are confident that these enhancements reflect real increases in the atmospheric XCO_2. The measurement site is located in an urban area; it is surrounded by several coal- and gas power plants. The closest ones are in the town Karlsruhe (13 km to the South-West with 915 MW), in Mannheim (39 km to the North with 1675 MW) and in Heilbronn (57 km to the East with 950 WM). On the 28 March, the wind came from the North, so we suspect the increases of CO_2 originated from the power plant in the city of Mannheim.

A slight air mass dependent difference is visible between the 4 datasets. It is nearly negligible between the 2 low-resolution datasets and biggest between the "EM27" and the

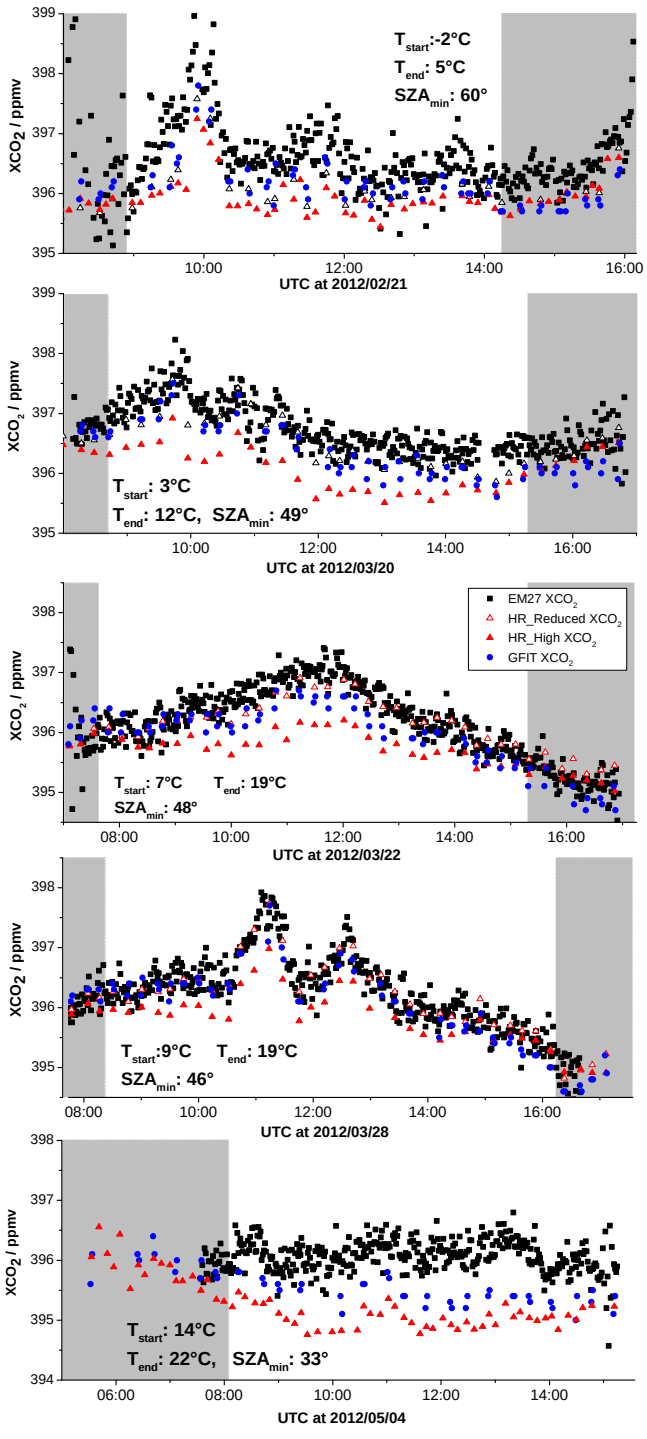

Fig. 8. Measurements of retrieved XCO_2 at 5 sample days. The number of interferograms and respective recording time contained in a single datapoint of each type are the same than in Fig. 6

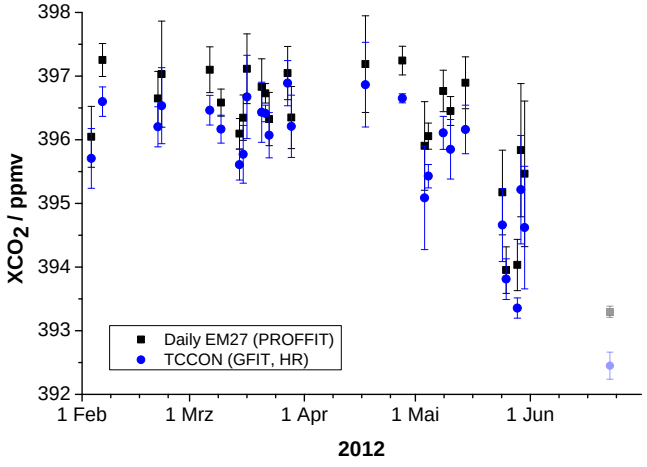

Fig. 9. Daily means of XCO_2 values of the EM27 and the TCCON instrument. The last day is preliminary only.

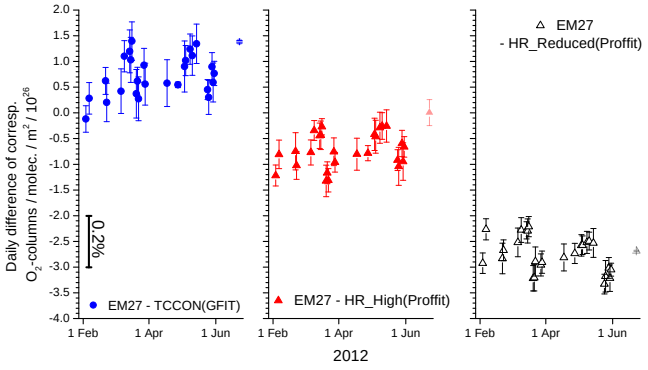

Fig. 10. Differences between the EM27 O_2 total columns and the 3 other datasets, where the daily means of the differences with the according 1-σ error bars are shown. To obtain the differences, only IFGs were taken into account, which were recorded at the same time. The last day is preliminary only and not taken into account in the statistical evaluation.

"HR_High". However, it is worth mentioning that these effects are below 0.25 % and could essentially be shifted into an airmass-dependent post-correction.

5.3 Comparisons

To compare the XCO_2-results over the whole time series of 26 measurement days between February and May 2012, we calculated the daily means which are shown in Fig. 9.

As the 1-σ error bars for the daily mean values mainly result from the intraday variabilities, a more significant comparison can be done by calculating the differences between the "EM27" values and the three other data types "GFIT", "HR_High" and "HR_Reduced" (see Sect. 4.2). To reduce temporal variabilities, only data were taken into account, which were recorded at nearly the same time. In addition, as described above, only measurements were taken into account which had a corresponding SZA lower than 70 ° and were taken at least 30 min after the set-up of the instrument on the terrace. For one datapoint taken with the HR instrument (duration 212 s, containing 2 forward and 2 backward IFGs), the data of 3 EM27 spectra (total measurement duration 102 s; each spectrum containing 10 IFGs) were averaged and used. As we alternately recorded 0.5 cm^{-1} and 1 cm^{-1} spectra as described in Sect. 4.1, these 3 EM27 0.5 cm^{-1} measurements span about the same time period as the measurement time of an HR-datapoint (average of 2 forward and 2 backward IFGs).

Following this procedure, the XCO_2 and the total O_2 column values are investigated in the following. The O_2 column values offer the advantage that there is no significant variability on short time scales which could superimpose the instrumental effects under investigation.

In Fig. 10 the statistical behaviour of the O_2 column differences for each measurement day are collected. The mean difference, and the 1-σ error bar according to the intraday scatter is shown. These daily means are made only for graphical reasons and not for the following statistical values. For all simultaneously measured results in the whole time series, the differences in the O_2 columns have the following values:

EM27-GFIT: $(7 \pm 5) \times 10^{25}\,\mathrm{molec\,m^{-2}}$
$\widehat{=}(0.15 \pm 0.11)\,\%$

EM27-HR_High: $(-7 \pm 4) \times 10^{25}\,\mathrm{molec\,m^{-2}}$
$\widehat{=}(-0.15 \pm 0.09)\,\%$

EM27-HR_Reduced: $(-27 \pm 4) \times 10^{25}\,\mathrm{molec\,m^{-2}}$
$\widehat{=}(-0.59 \pm 0.09)\,\%$

The mean differences show significant offsets, as already discussed in Sect. 5.1. However, they compensate for the largest part when calculating the XCO_2. The scatter around the mean systematic offset, the precision, is impressively good with values around 0.1 %, proving the high stability of the EM27 instrument.

When moving on to the XCO_2, one obtains results as shown in Fig. 11 and the following statistical values:

EM27-GFIT: (0.46 ± 0.32) ppm
$\widehat{=}(0.12 \pm 0.08)\,\%$

EM27-HR_High: (0.81 ± 0.36) ppm
$\widehat{=}(0.20 \pm 0.09)\,\%$

EM27-HR_Reduced: (0.26 ± 0.29) ppm
$\widehat{=}(0.07 \pm 0.07)\,\%$

These values show a very good accuracy of better than 0.2 % relative to a high-resolution instrument. We believe, that these could be absorbed by a global scaling factor for a hypothetical EM27 network (and an airmass-dependent correction term for reaching even higher accuracies), similar to the WMO factor which is applied to the TCCON XCO_2 values,

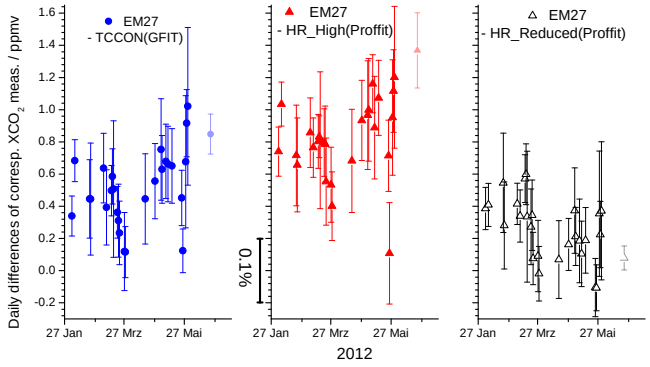

Fig. 11. XCO_2 values with the same data processing as for the O_2 columns in Fig. 10 for the 26 measurement days.

presuming the low-resolution instruments are all identical in construction. The scattering between the EM27 and the high-resolution data is lower than 0.09 %, well inside the range of the stated precision of the TCCON network which is 0.25 % (Wunch et al., 2011).

5.4 XCO_2-signal to noise

To approximately compare the signal-to-noise of the XCO_2-values, we applied a running average to the EM27 and GFIT(TCCON) values of a few days (see Fig. 12 for 22 March 2012) and calculated the scatter of the data. The GFIT values show a standard deviation of 0.085 ppm for a recording time of 212 s (average of 2 forward and 2 backward scans). The EM27 values which had a recording time of 34 s per datapoint in Fig. 12 (which includes 10 scans) have a 1σ standard deviation of 0.17 ppm. For an acquisition time of 212 s this value lies at approximately $0.17\,\text{ppm} \cdot \sqrt{34\,\text{s}/212\,\text{s}} = 0.07\,\text{ppm}$, which is comparable to the GFIT(TCCON) value. On first sight this is surprising when having in mind the very small parallel beam diameter of 3 mm of the EM27. In total, the intensity on the EM27 detector is a factor of about 150 smaller than on the HR detector. However, the photon noise part of the Signal-to-Noise Ratio (SNR) of an FTIR spectrum also is dependent on the resolution, or more precisely the number N of datapoints in the interferogram. This factor of $\sqrt{2/N}$ leads to a comparable SNR of the low-resolution measurements.

6 Conclusions

We presented the capabilities of retrieving atmospheric XCO_2 values with a NIR-modified version of the commercial EM27 FTIR spectrometer from Bruker, a low-resolution table top FTS. We developed a small solar tracker with active control of the line-of-sight, which is attached to the spectrometer. The whole set-up is very portable.

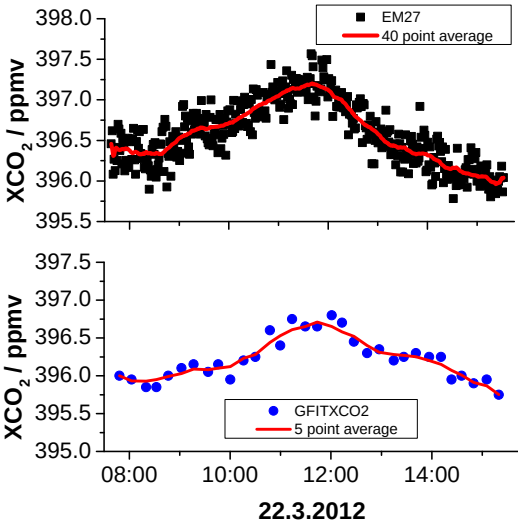

Fig. 12. Sample day to derive the XCO_2 noise of the EM27 and GFIT(TCCON) values. When taking into account the different recording durations, the noise level is comparable. The number of interferograms and respective recording time contained in a single EM27 datapoint are 10 IFGs and 34 s, for a single GFIT datapoint 4 IFGs and 212 s.

To confirm the resulting data quality, we compared the EM27 results with simultaneously recorded measurements of the high-resolution TCCON FTIR spectrometer located in the vicinity of the test setup.

This intercomparison demonstrates for the first time the applicability of a well-characterised low-resolution FTS spectrometer for XCO_2 measurements. The precision of the EM27 values found in this investigation is well inside the current network-wide TCCON accuracy of 0.25 %. The differences of temporally coinciding measurements for the retrieved XCO_2 were (0.12 ± 0.08) % and (0.20 ± 0.09) % when compared to high-resolution TCCON spectra, analysed with the official GFIT and PROFFIT algorithms, respectively. The optical stability and the low influence of varying outside temperatures (-10 °C to more than 40 °C) are promising features of the EM27 spectrometer, so our study proves its applicability especially for operation at remote sites and measurement campaigns.

Therefore, the EM27, with the modifications presented in this paper, seems a very promising candidate for an instrument supporting the core TCCON stations for increasing the global representativeness of greenhouse gas measurements by the operation of EM27 spectrometers at places inaccessible with a TCCON spectrometer. Moreover, for the study of local emission sources as megacities, large power plants, etc., several mobile EM27 units could be distributed.

Acknowledgements. M. Gisi has been partially funded through grant BU2599/1-1 (RemoteC, http://www.imk-asf.kit.edu/english/RemoteC.php) within the Emmy-Noether programme of Deutsche Forschungsgemeinschaft (DFG).

We acknowledge Martin Kohler from the "Institute for Meteorology and Climate Research – Troposphere Research (IMK-TRO)" at the KIT for providing tall-tower meteorological data.

We acknowledge the Global Modelling and Assimilation Office (GMAO) and the GES DISC for the dissemination of MERRA meteorological datasets.

We acknowledge support by Deutsche Forschungsgemeinschaft and Open Access Publishing Fund of Karlsruhe Institute of Technology.

The service charges for this open access publication have been covered by a Research Centre of the Helmholtz Association.

Edited by: J. Notholt

References

Chen, J., Gottlieb, E., and Wofsy, S.: Compact FTIR Spectrometer for total column measurement in urban environments, in: IRWG/TCCON Meeting, Wengen, Switzerland, 11–15 June 2012.

Geibel, M. C., Gerbig, C., and Feist, D. G.: A new fully automated FTIR system for total column measurements of greenhouse gases, Atmos. Meas. Tech., 3, 1363–1375, doi:10.5194/amt-3-1363-2010, 2010.

Gisi, M., Hase, F., Dohe, S., and Blumenstock, T.: Camtracker: a new camera controlled high precision solar tracker system for FTIR-spectrometers, Atmos. Meas. Tech., 4, 47–54, doi:10.5194/amt-4-47-2011, 2011.

Hase, F.: Improved instrumental line shape monitoring for the ground-based, high-resolution FTIR spectrometers of the Network for the Detection of Atmospheric Composition Change, Atmos. Meas. Tech., 5, 603–610, doi:10.5194/amt-5-603-2012, 2012.

Hase, F., Blumenstock, T., and Paton-Walsh, C.: Analysis of the instrumental line shape of high-resolution fourier transform IR spectrometers with gas cell measurements and new retrieval software, Appl. Optics, 38, 3417–3422, doi:10.1364/AO.38.003417, 1999.

Hase, F., Demoulin P., Sauval, A. J., Toon, G. C., Bernath, P. F., Goldman, A., Hannigan, J. W., and Rinsland, C. P.: An empirical line-by-line model for the infrared solar transmittance spectrum from 700 to 5000 cm-1, J. Quant. Spectr. Radiative Trans., 102, 450–463, doi:10.1016/j.jqsrt.2006.02.026, 2006.

Jones, N., Griffith, D., Velazco, V., Macatangay, R., O'Brien, D., Clark, A., and Rayner, P.: SolarFTS-lite down under, in: IRWG/TCCON Meeting, Wengen, Switzerland, 11–15 June 2012.

Keppel-Aleks, G., Toon, G. C., Wennberg, P. O., and Deutscher, N. M.: Reducing the impact of source brightness fluctuations on spectra obtained by Fourier-transform spectrometry, Appl. Optics, 46, 4774–4779, doi:10.1364/AO.46.004774, 2007.

Kobayashi, N., Inoue, G., Kawasaki, M., Yoshioka, H., Minomura, M., Murata, I., Nagahama, T., Matsumi, Y., Tanaka, T., Morino, I., and Ibuki, T.: Remotely operable compact instruments for measuring atmospheric CO_2 and CH_4 column densities at surface monitoring sites, Atmos. Meas. Tech., 3, 1103–1112, doi:10.5194/amt-3-1103-2010, 2010.

Lamouroux, J., Tran, H., Laraia, A. L., Gamache, R. R., Rothman, L. S., Gordon, I. E., and Hartmann, J. M.: Updated database plus software for line-mixing in CO_2 infrared spectra and their test using laboratory spectra in the 1.5–2.3 µm region, J. Quant. Spectrosc. Ra., 111, 2321–2331, doi:10.1016/j.jqsrt.2010.03.006, 2010.

Messerschmidt, J., Macatangay, R., Notholt, J., Petri, C., Warneke, T., and Weinzierl, C.: Side by side measurements of CO_2 by ground-based Fourier transform spectrometry (FTS), Tellus B, 62, 749–758, doi:10.1111/j.1600-0889.2010.00491.x, 2010.

Messerschmidt, J., Geibel, M. C., Blumenstock, T., Chen, H., Deutscher, N. M., Engel, A., Feist, D. G., Gerbig, C., Gisi, M., Hase, F., Katrynski, K., Kolle, O., Lavrič, J. V., Notholt, J., Palm, M., Ramonet, M., Rettinger, M., Schmidt, M., Sussmann, R., Toon, G. C., Truong, F., Warneke, T., Wennberg, P. O., Wunch, D., and Xueref-Remy, I.: Calibration of TCCON column-averaged CO_2: the first aircraft campaign over European TCCON sites, Atmos. Chem. Phys., 11, 10765–10777, doi:10.5194/acp-11-10765-2011, 2011.

Notholt, J., Toon, G., Rinsland, C., Pougatchev, N., Jones, N., Connor, B., Weller, R., Gautrois, M., and Schrems, O.: Latitudinal variations of trace gas concentrations in the free troposphere measured by solar absorption spectroscopy during a ship cruise, J. Geophys. Res.-Atmos., 105, 1337–1349, doi:10.1029/1999JD900940, 2000.

Olsen, S. C. and Randerson, J. T.: Differences between surface and columnatmospheric CO_2 and implications for carbon cycle research, J. Geophys.Res., 109, D02301, doi:10.1029/2003JD003968, 2004.

Petri, C., Warneke, T., Jones, N., Ridder, T., Messerschmidt, J., Weinzierl, T., Geibel, M., and Notholt, J.: Remote sensing of CO_2 and CH_4 using solar absorption spectrometry with a low resolution spectrometer, Atmos. Meas. Tech., 5, 1627–1635, doi:10.5194/amt-5-1627-2012, 2012.

Schneider, M., Hase, F., Blumenstock, T., Redondas, A., and Cuevas, E.: Quality assessment of O_3 profiles measured by a state-of-the-art ground-based FTIR observing system, Atmos. Chem. Phys., 8, 5579–5588, doi:10.5194/acp-8-5579-2008, 2008.

Schneider, M., Romero, P. M., Hase, F., Blumenstock, T., Cuevas, E., and Ramos, R.: Continuous quality assessment of atmospheric water vapour measurement techniques: FTIR, Cimel, MFRSR, GPS, and Vaisala RS92, Atmos. Meas. Tech., 3, 323–338, doi:10.5194/amt-3-323-2010, 2010.

Sepúlveda, E., Schneider, M., Hase, F., García, O. E., Gomez-Pelaez, A., Dohe, S., Blumenstock, T., and Guerra, J. C.: Long-term validation of tropospheric column-averaged CH_4 mole fractions obtained by mid-infrared ground-based FTIR spectrometry, Atmos. Meas. Tech., 5, 1425–1441, doi:10.5194/amt-5-1425-2012, 2012.

Wunch, D., Toon, G. C., Wennberg, P. O., Wofsy, S. C., Stephens, B. B., Fischer, M. L., Uchino, O., Abshire, J. B.,

Bernath, P., Biraud, S. C., Blavier, J.-F. L., Boone, C., Bowman, K. P., Browell, E. V., Campos, T., Connor, B. J., Daube, B. C., Deutscher, N. M., Diao, M., Elkins, J. W., Gerbig, C., Gottlieb, E., Griffith, D. W. T., Hurst, D. F., Jiménez, R., Keppel-Aleks, G., Kort, E. A., Macatangay, R., Machida, T., Matsueda, H., Moore, F., Morino, I., Park, S., Robinson, J., Roehl, C. M., Sawa, Y., Sherlock, V., Sweeney, C., Tanaka, T., and Zondlo, M. A.: Calibration of the Total Carbon Column Observing Network using aircraft profile data, Atmos. Meas. Tech., 3, 1351–1362, doi:10.5194/amt-3-1351-2010, 2010.

Wunch, D., Toon, G. C., Blavier, J.-F. L., Washenfelder, R. A., Notholt, J., Connor, B. J., Griffith, D. W. T., Sherlock, V., and Wennberg, P. O.: The Total Carbon Column Observing Network, Philos. T. Roy. Soc. A, 369, 2087–2112, doi:10.1098/rsta.2010.0240, 2011.